

# Comparison of the color-evaporation model and the NRQCD factorization approach in charmonium production

Geoffrey T. Bodwin,<sup>1</sup> Eric Braaten,<sup>2</sup> and Jungil Lee<sup>3</sup>

<sup>1</sup> *High Energy Physics Division, Argonne National Laboratory,  
9700 South Cass Avenue, Argonne, Illinois 60439*

<sup>2</sup> *Physics Department, Ohio State University, Columbus, Ohio 43210*

<sup>3</sup> *Department of Physics, Korea University, Seoul 136-701, Korea*

(Dated: December 24, 2018)

## Abstract

We compare the color-evaporation model (CEM) and nonrelativistic QCD (NRQCD) factorization predictions for inclusive quarkonium production. Using the NRQCD factorization formulas for quarkonium production and for perturbative  $Q\bar{Q}$  production, we deduce relationships that are implied by the CEM between the nonperturbative NRQCD matrix elements that appear in the factorization formula for quarkonium production. These relationships are at odds with the phenomenological values of the matrix elements that have been extracted from the Tevatron data for charmonium production at large transverse momentum. A direct comparison of the CEM and NRQCD factorization predictions with the CDF charmonium production data reveals that the CEM fits to the data are significantly worse than the NRQCD factorization fits. The inclusion of  $k_T$  smearing improves the CEM fits substantially, but the  $k_T$ -smearred NRQCD factorization fits are superior. The NRQCD factorization fits to the  $\chi_c$  data indicate that multiple gluon radiation is an essential ingredient in obtaining the correct shape of the cross section as a function of  $p_T$ .

PACS numbers: 14.40.Gx,13.85.Ni,12.38.-t,12.38.Bx

## I. INTRODUCTION

In general, the production rates for specific hadronic states in high-energy processes are difficult to understand from first principles because they involve nonperturbative aspects of QCD in an essential way. The inclusive production rates for heavy quarkonium states have two aspects that facilitate their understanding from first principles. First, the mass  $m_Q$  of the heavy quark and the antiquark that are the constituents of the quarkonium are large compared to the scale  $\Lambda_{\text{QCD}}$  that is associated with the nonperturbative aspects of QCD. Second, the inclusive nature of the quarkonium production process may make it less sensitive, at transverse momenta  $p_T$  that are much greater than  $\Lambda_{\text{QCD}}$ , to nonperturbative effects that are associated with the formation of color-singlet hadrons from the colored partons.

Two models for the inclusive production of heavy quarkonium were introduced in the 1970's: the color-singlet model (CSM) and the color-evaporation model (CEM). These models make very different assumptions about the rôles played by the colors and spins of the heavy quark and antiquark in the production process. In the CSM, it is assumed that a specific quarkonium state can be formed only if the  $Q\bar{Q}$  pair is created in a color-singlet state with the same angular momentum quantum numbers as the quarkonium. In the CEM, the probability of forming a specific quarkonium state is assumed to be independent of the color of the  $Q\bar{Q}$  pair. In some versions of the CEM, the probability of forming a specific quarkonium state is also assumed to be independent of the spin of the  $Q\bar{Q}$  pair. In spite of the very different assumptions that are made in the CSM and CEM, both models enjoyed considerable phenomenological success through the 1980's and into the 1990's.

In 1995, a new approach for describing inclusive heavy quarkonium production based on first principles was developed: the NRQCD factorization approach [1]. It makes use of an effective field theory called nonrelativistic QCD (NRQCD) [2, 3] to exploit the large mass of the heavy quark, and it further assumes that, owing to the inclusive nature of the production process, traditional factorization methods can be exploited to establish a factorization formula. The NRQCD factorization approach incorporates aspects of both the CSM and CEM and can be regarded as a unification of these two models within a consistent theoretical framework. It can be summarized by the NRQCD factorization formula, which separates short-distance, perturbative effects involving momenta of order  $m_Q$  from long-distance, nonperturbative effects.

The nonperturbative factors in the NRQCD factorization formula are NRQCD matrix elements. NRQCD can be used to give rough predictions of the relative sizes of the matrix elements. These predictions are based on the leading power behavior of the matrix elements as a function of the typical heavy-quark velocity  $v$  in the quarkonium rest frame. In order to obtain an estimate, one makes the assumption that, for each matrix element, the coefficient of the leading power of  $v$  is of order unity. This last assumption may not be reliable. However, one can ignore this  $v$ -scaling information and treat the NRQCD factorization formula as a general phenomenological framework for analyzing inclusive heavy quarkonium production. Any model that can be described in terms of QCD processes at short distances, including the CSM and the CEM, can be formulated in terms of assumptions about the matrix elements in the NRQCD factorization formula.

In this paper, we derive relationships between the NRQCD nonperturbative factors that follow from the model assumptions of the CEM. We find that these relationships are often poorly satisfied by phenomenological values of the NRQCD matrix elements. Furthermore, the relationships sometimes violate the  $v$ -scaling rules of NRQCD themselves. We conclude

that the CEM and NRQCD provide very different pictures of the evolution of a heavy quark-antiquark pair into a quarkonium.

Using existing data, CSM can be excluded as a quantitative model of heavy-quarkonium production. In 1995, the CDF collaboration measured the cross sections for the prompt production of  $J/\psi$  and  $\psi(2S)$  in  $p\bar{p}$  collisions at a center-of-mass energy of 1.8 TeV. It discovered that the cross sections are more than an order-of-magnitude larger than those predicted by the CSM. This dramatic discrepancy eliminated the CSM as a viable model for inclusive heavy quarkonium production. (A detailed discussion of these comparisons between the CSM and the experimental data and references to the published experimental results and theoretical results can be found in Ref. [4].)

The CEM can also be ruled out on the basis of the simple qualitative prediction that the ratio of the inclusive production rates for any two quarkonium states should be independent of the process. The most dramatic violation of this prediction that has been observed is in the fraction of  $J/\psi$ 's that come from decays of the  $P$ -wave charmonium states  $\chi_{c1}$  and  $\chi_{c2}$ . This fraction is measured to be  $0.11 \pm 0.02$  in  $B$  decays and  $0.297 \pm 0.017_{\text{stat}} \pm 0.057_{\text{sys}}$  for prompt production at the Fermilab Tevatron. The version of the CEM in which the probability for the formation of a quarkonium is assumed to be independent of the spin state of the  $Q\bar{Q}$  pair can be ruled out on the basis of several other simple qualitative predictions. One such prediction is that the inclusive production rate of a quarkonium state should be independent of its spin state, so that it should always be produced unpolarized. This prediction is contradicted by the observation of nonzero polarization of  $J/\psi$ 's in  $e^+e^-$  annihilation at the  $B$  factories and by the observation of nonzero polarization of the bottomonium states  $\Upsilon(2S)$  and  $\Upsilon(3S)$  in a fixed-target experiment. A further prediction of this version of the CEM is that the production rates for the  $P$ -wave charmonium state  $\chi_{cJ}$  should be proportional to  $2J + 1$ , and, hence, that the ratio of the inclusive cross sections for  $\chi_{c1}$  and  $\chi_{c2}$  production should be  $3/5$ . For prompt production at the Tevatron, this ratio has been measured to be  $1.04 \pm 0.29_{\text{stat}} \pm 0.12_{\text{sys}}$ . (A detailed discussion of these comparisons between the CEM and the experimental data and references to the published experimental results and theoretical results can be found in Ref. [4].)

Since the CEM is only a model, it can be salvaged simply by declaring it to have a limited domain of applicability. The failure of the predictions for polarization can be avoided by declaring the model to apply only to cross sections that are summed over the spin states of the quarkonium. In the case of the predictions that ratios of quarkonium cross sections should be the same for all processes, the most dramatic failures can be avoided by declaring the model to apply only when the total hadronic energy is sufficiently large. This condition can be used to exclude applications to  $B$  decays and to  $e^+e^-$  annihilation at  $\sqrt{s} = 10.6$  GeV. In this case, the CEM reduces essentially to a model for inclusive production of quarkonium, without regard to spin, in high energy fixed-target experiments,  $p\bar{p}$  collisions at the Tevatron, and  $pp$  collisions at the LHC.

It may be possible to exclude even this limited version of the CEM, given sufficiently accurate experimental information. In this paper, we present a quantitative comparison of the predictions of the CEM and the NRQCD factorization approach for transverse momentum distributions of heavy quarkonium at the Tevatron. We restrict our attention to the region of transverse momentum comparable to or larger than the quarkonium mass, where the effects of multiple-soft gluon emission are not so important. We find that the NRQCD factorization approach gives a significantly better fit to the available data.

The remainder of this paper is organized as follows. In Sec. II, we describe the NRQCD

factorization formula for quarkonium production and the  $v$ -scaling rules for the NRQCD matrix elements. In Sec. III, we describe the CEM, use the NRQCD factorization formula to derive expressions for the ratios of NRQCD matrix elements that are implied by the CEM assumptions, and deduce the  $v$ -scaling rules that follow from these ratios. Sec. IV contains a comparison of the ratios implied by the CEM with the ratios of phenomenological matrix elements that have been extracted from the Tevatron data for  $J/\psi$  and  $\psi(2S)$  production. Sec. IV also contains a direct comparison of fits of the CEM predictions and the NRQCD factorization predictions to the Tevatron data. Sec. V contains similar comparisons for  $\chi_c$  production. Finally, we present our conclusions in Sec. VI.

## II. NRQCD FACTORIZATION FORMULA

The NRQCD factorization formula for the inclusive cross section for production of a specific heavy-quarkonium state  $H$  is

$$\sigma[AB \rightarrow H + X] = \sum_n c_n^{AB}(\Lambda) \langle \mathcal{O}_n^H(\Lambda) \rangle. \quad (1)$$

Here,  $A$  and  $B$  are light hadrons, photons, or leptons, and  $\Lambda$  is the ultraviolet cutoff of the effective theory. The  $c_n^{AB}$  are short-distance coefficients that can be calculated in perturbation theory by matching amplitudes in NRQCD with those in full QCD. The matrix elements  $\langle \mathcal{O}_n^H \rangle$  are vacuum-expectation values of four-fermion operators in NRQCD, evaluated in the rest frame of the quarkonium. These matrix elements contain all of the nonperturbative physics of the evolution of a  $Q\bar{Q}$  into a quarkonium state. The operators have the form

$$\mathcal{O}_n^H = \chi^\dagger \kappa_n \psi \mathcal{P}^H(\Lambda) \psi^\dagger \kappa'_n \chi, \quad (2)$$

where  $\psi$  is the two-component (Pauli) spinor that annihilates a heavy quark,  $\chi$  is the two-component spinor that creates a heavy antiquark, and  $\mathcal{P}^H$  is a projector onto states that in the asymptotic future contain the quarkonium  $H$  plus light partons  $X$  whose energies and momenta lie below the cutoff  $\Lambda$  of the effective field theory:

$$\mathcal{P}^H(\Lambda) = \sum_X |H + X, t \rightarrow \infty\rangle \langle H + X, t \rightarrow \infty|. \quad (3)$$

The factors  $\kappa_n$  and  $\kappa'_n$  in Eq. (2) are direct products of a color matrix (either the unit matrix or the matrix  $T^a$  with octet index  $a$ ), a spin matrix (either the unit matrix or the matrix  $\sigma^i$  with triplet index  $i$ ), and a polynomial in the QCD covariant derivative  $\mathbf{D} = \nabla + ig\mathbf{A}$  and the QCD field strengths. The NRQCD factorization formula in Eq. (1) was proposed in Ref. [1]. Some hard-scattering factorization formulas, such as those for deep-inelastic scattering, Drell-Yan lepton-pair production, and  $e^+e^-$  annihilation into hadrons, have been proven to hold to all orders in the strong coupling  $\alpha_s$ . The derivation of the NRQCD factorization formula is not at this level of rigor.<sup>1</sup> However, in this regard it is no different

---

<sup>1</sup> A recent study of certain two-loop contributions to quarkonium production [5] has revealed that, if factorization is to hold, then the color-octet NRQCD production matrix elements must be modified from the form given in Eq. (2) by the inclusion of light-like eikonal lines that run from each of the  $Q\bar{Q}$  bilinears to the far future. It is not known if this modification preserves the factorized form in higher orders.

TABLE I: Velocity-suppression factors for NRQCD matrix elements in  $S$ -wave and  $P$ -wave  $Q\bar{Q}$  channels in NRQCD and in the CEM. The 1 or 8 indicates the color channel and  $^{2s+1}L_j$  indicates the angular-momentum channel. For NRQCD, the  $v$ -suppression factors up to order  $v^4$  are given for representative  $S$ -wave and  $P$ -wave multiplets. For the CEM, the orders of the  $v$ -suppression factors are independent of the quarkonium state  $H$ , as described in Sec. III.

	$1, ^1S_0$	$1, ^3S_1$	$8, ^1S_0$	$8, ^3S_1$	$1, ^1P_1$	$1, ^3P_0$	$1, ^3P_1$	$1, ^3P_2$	$8, ^1P_1$	$8, ^3P_0$	$8, ^3P_1$	$8, ^3P_2$
NRQCD Factorization												
$\eta_c$	1		$v^4$	$v^3$					$v^4$			
$J/\psi$		1	$v^3$	$v^4$						$v^4$	$v^4$	$v^4$
$h_c$			$v^2$		$v^2$							
$\chi_{c0}$				$v^2$		$v^2$						
$\chi_{c1}$				$v^2$			$v^2$					
$\chi_{c2}$				$v^2$				$v^2$				
Color-Evaporation Model												
$H$	1	1	1	1	$v^2$							

from the factorization formula for semi-inclusive production of a hadron in hadron-hadron collisions. The existing all-orders proofs of factorization formulas require that the observed scattered particle be produced at a large transverse momentum compared with the QCD scale  $\Lambda_{\text{QCD}}$  and that the cross section be sufficiently inclusive. ‘‘Sufficiently inclusive’’ means that the variables in which the cross section is differential cannot assume values that restrict final-state parton momenta in the parton-level cross section to be within order  $\Lambda_{\text{QCD}}$  of soft or collinear singularities.

The matrix elements in Eq. (1) fall into a hierarchy according to their scaling with the velocity  $v$  of the heavy quark (or antiquark) in the quarkonium rest frame.  $v^2 \approx 0.3$  for charmonium, and  $v^2 \approx 0.1$  for bottomonium. In practice, the summation over these matrix elements is usually truncated at a low order in  $v$ . The NRQCD factorization formalism has enjoyed a good deal of phenomenological success in describing inclusive quarkonium production at hadron,  $ep$ , and  $e^+e^-$  colliders and in fixed-target experiments.<sup>2</sup>

A standard set of the NRQCD operators  $\mathcal{O}_n^H$  that appear naturally in cross sections that are summed over the spin states of the quarkonium was introduced in Ref. [1]. They are denoted by  $\mathcal{O}_1^H(^{2s+1}L_j)$  and  $\mathcal{O}_8^H(^{2s+1}L_j)$ , where the subscript indicates the color state of the  $Q\bar{Q}$  pair (1 for singlet and 8 for octet), and the argument indicates the angular-momentum state of the  $Q\bar{Q}$  pair ( $s$  is the total spin quantum number,  $L = S, P, \dots$  indicates the orbital-angular-momentum quantum number, and  $j$  is the total-angular-momentum quantum number). There are implied sums over the spin states of the quarkonium  $H$ .

The velocity-scaling rules of NRQCD imply an intricate pattern of suppression factors for the NRQCD matrix elements  $\langle \mathcal{O}_n^H \rangle$ . The suppression factors, up to order  $v^4$  for  $S$ -wave and  $P$ -wave  $Q\bar{Q}$  channels, are given in Table I for the representative  $S$ -wave multiplet that consists of the charmonium states  $\eta_c$  and  $J/\psi$  and for the representative  $P$ -wave charmonium multiplet that consists of the charmonium states  $h_c$ ,  $\chi_{c0}$ ,  $\chi_{c1}$ , and  $\chi_{c2}$ .

<sup>2</sup> See Ref. [4] for a recent summary of the phenomenology of quarkonium production.

### III. COLOR-EVAPORATION MODEL

The color-evaporation model (CEM) was first proposed in 1977 [6–9]. In the CEM, the cross section for a quarkonium state  $H$  is some fraction  $F_H$  of the cross section for producing  $Q\bar{Q}$  pairs with invariant mass below the  $M\bar{M}$  threshold, where  $M$  is the lowest-mass meson containing the heavy quark  $Q$ . The fractions  $F_H$  are assumed to be universal so that, once they are determined by data, they can be used to predict the cross sections in other processes and in other kinematic regions. The cross section for producing  $Q\bar{Q}$  pairs that is used in the CEM has an upper limit on the  $Q\bar{Q}$  pair mass, but no constraints on the color or spin of the final state. The  $Q\bar{Q}$  pair is assumed to neutralize its color by interaction with the collision-induced color field, that is, by “color evaporation.” In some versions of the CEM [10], the color-neutralization process is also assumed to randomize the spins of the  $Q$  and the  $\bar{Q}$ . The CEM parameter  $F_H$  is the probability that a  $Q\bar{Q}$  pair with invariant mass less than  $2m_M$ , where  $m_M$  is the mass of the meson  $M$ , will bind to form the quarkonium  $H$ . That probability is assumed to be 0 if the  $Q\bar{Q}$  pair has invariant mass greater than  $2m_M$ .

In the CEM, the production cross section for the quarkonium state  $H$  in collisions of the light hadrons, photons, or leptons  $A$  and  $B$  is

$$\sigma_{\text{CEM}}[AB \rightarrow H + X] = F_H \int_{4m^2}^{4m_M^2} dm_{Q\bar{Q}}^2 \frac{d\sigma}{dm_{Q\bar{Q}}^2}[AB \rightarrow Q\bar{Q} + X], \quad (4)$$

where  $m_{Q\bar{Q}}$  is the invariant mass of the  $Q\bar{Q}$  pair,  $m$  is the heavy-quark mass, and  $d\sigma/dm_{Q\bar{Q}}^2$  on the right side is the inclusive differential cross section for a  $Q\bar{Q}$  pair to be produced in a collision of  $A$  and  $B$ . There is an implied sum over the colors and spins of the final-state  $Q\bar{Q}$  pair. This is where the central model assumptions of color evaporation and spin randomization manifest themselves.

If  $A$  and/or  $B$  are hadrons or photons, the cross section for  $AB \rightarrow Q\bar{Q} + X$  can be expressed as convolutions of parton distributions for  $A$  and/or  $B$  and a parton cross section. At leading order in  $\alpha_s$ , the parton process  $ij \rightarrow Q\bar{Q}$  creates a  $Q\bar{Q}$  pair with zero transverse momentum, and the differential cross section  $d\sigma/dp_T^2$  is proportional to  $\delta(p_T^2)$ . At next-to-leading order in  $\alpha_s$  (NLO), there are parton processes  $ij \rightarrow Q\bar{Q} + k$  that create a  $Q\bar{Q}$  pair with nonzero  $p_T$ . The complete NLO differential cross section is a distribution that includes singular terms proportional to  $\delta(p_T^2)$  and  $1/p_T^2$ , but whose integral over  $p_T^2$  is well behaved. Some kind of smearing over  $p_T$  is necessary to obtain a smooth  $p_T$  distribution that can be compared with experiment. The physical origin of the smearing is multiple gluon emission from the initial- and final-state partons. A rigorous treatment of the effects of multiple gluon emission requires the resummation of logarithmic corrections to all orders in  $\alpha_s$  [11–13]. A simple phenomenological model for the effects of multiple gluon emission is  $k_T$  smearing, in which the colliding partons are given Gaussian distributions in the intrinsic transverse momentum with a width  $\langle k_T^2 \rangle$  that is treated as a phenomenological parameter.

Complete NLO calculations of quarkonium production in hadronic collisions using the CEM have been carried out in Refs. [14, 15], using the exclusive  $Q\bar{Q}$  production code of Ref. [16] to obtain the  $Q\bar{Q}$  pair distributions. There are also calculations in the CEM beyond LO that use only a subset of the NLO diagrams [10] and calculations that describe the soft color interaction within the framework of a Monte Carlo event generator [17]. Calculations beyond LO in the CEM have also been carried out for  $\gamma p$ ,  $\gamma\gamma$ , and neutrino-nucleon collisions and for  $Z$  decays [18–22].

We now proceed to elucidate the relationship between the CEM and the NRQCD factorization formula. According to the NRQCD factorization formalism, the differential cross section for the process  $AB \rightarrow Q\bar{Q} + X$  is given by

$$\frac{d\sigma}{dm_{Q\bar{Q}}^2}[AB \rightarrow Q\bar{Q} + X] = \sum_n c_n^{AB} \sum_{\text{spins}} \sum_{\text{colors}} \int \frac{d^3k}{(2\pi)^3} \langle \mathcal{O}_n^{Q(+\mathbf{k})\bar{Q}(-\mathbf{k})} \rangle \delta[m_{Q\bar{Q}}^2 - 4(\mathbf{k}^2 + m^2)], \quad (5)$$

where the  $c_n^{AB}$  are the same short-distance coefficients that appear in Eq. (1). We have suppressed the dependence of the coefficients and the operators on the ultraviolet cutoff  $\Lambda$  of the effective field theory. The operator  $\mathcal{O}_n^{Q(+\mathbf{k})\bar{Q}(-\mathbf{k})}$  is analogous to the operator in Eq. (2), except that the quarkonium state  $H$  is replaced by a perturbative state that consists of a  $Q$  and a  $\bar{Q}$  with momenta  $\pm\mathbf{k}$  and with definite spin and color indices that have been suppressed. Those suppressed indices are summed over in Eq. (5). It is convenient to define a  $Q\bar{Q}$  operator that includes the sum over the colors and spins and an average over the directions of the momenta  $\pm\mathbf{k}$  of the  $Q$  and  $\bar{Q}$ :

$$\mathcal{O}_n^{Q\bar{Q}}(k) = \chi^\dagger \kappa_n \psi \left( \int \frac{d\Omega_k}{4\pi} \sum_{\text{spins}} \sum_{\text{colors}} \mathcal{P}^{Q(+\mathbf{k})\bar{Q}(-\mathbf{k})} \right) \psi^\dagger \kappa'_n \chi, \quad (6)$$

where  $d\Omega_k$  is the element of angular integration of  $\mathbf{k}$  and  $k = |\mathbf{k}|$ .

Comparing Eqs. (1) and (4) and making use of Eq. (5), we see that the CEM implies that

$$\sum_n c_n^{AB} \langle \mathcal{O}_n^H \rangle = F_H \sum_n c_n^{AB} \frac{1}{2\pi^2} \int_0^{k_{\max}} k^2 dk \langle \mathcal{O}_n^{Q\bar{Q}}(k) \rangle, \quad (7)$$

where  $k_{\max} = \sqrt{m_M^2 - m^2}$ . Eq. (7) is the central relation that connects the NRQCD factorization approach with the CEM. If NRQCD factorization can be established to all orders in perturbation theory, then Eq. (7), which is a statement about the perturbative production of  $Q\bar{Q}$  states, must hold rigorously. This is to be contrasted with the NRQCD factorization approach itself, in which nonperturbative effects could conceivably spoil the factorization, even if the factorization formula can be established to all orders in perturbation theory. Note, however, that there is an implicit assumption in Eq. (7) that the sum over  $n$  converges. The sum need not converge rapidly in order to establish the relationship between the NRQCD factorization approach and the CEM, but it must converge. The expansion parameter in the sum is  $k_{\max}^2/m^2 \sim v^2$ . Hence, if the sum is to converge, we must have  $k_{\max}^2/m^2 \lesssim 1$ . In the charmonium system,  $M$  is the  $D$  meson, with mass 1.86 GeV. Taking  $m = 1.5$  GeV, we find that  $k_{\max}^2/m^2 \approx 0.54$ . In the bottomonium system,  $M$  is the  $B$  meson, with mass 5.28 GeV. Taking  $m = 4.7$  GeV, we find that  $k_{\max}^2/m^2 \approx 0.26$ . Thus the assumption  $k_{\max}^2/m^2 \lesssim 1$  is satisfied for the bottomonium system, but is only marginally satisfied for the charmonium system. There is also an implicit assumption that the energy of the produced quarkonium is not near the kinematic limit for the process. Near the kinematic limit, the  $v$  expansion of NRQCD breaks down, and, so, one needs to carry out a resummation of classes of NRQCD matrix elements in order to maintain the accuracy of the calculation [23]. Near the kinematic limit, the short-distance coefficients  $c_n^{AB}$  contain large logarithms that must be resummed as well [24].

Now we wish to establish that the equality in Eq. (7) must hold independently for each term in the sum over  $n$ . If we truncate the series at a finite number of terms, as is often done

in the phenomenology of quarkonium production, then the short-distance coefficients  $c_n^{AB}$  generally vary independently of each other as the kinematic variables of the incoming and outgoing particles vary. However, in some processes, for example, in quarkonium production as a function of  $p_T$  at the Tevatron, some of the short-distance coefficients show identical or nearly identical behavior as a function of the kinematic variable(s). Then one can establish the equality only of linear combinations of matrix elements. However, one can make a stronger assumption that the CEM must hold, not just for a particular quarkonium production process, but for all possible quarkonium production processes. Then, since Eq. (7) must hold for an arbitrarily large number of processes that have different short-distance coefficients, the equality in Eq. (7) must hold independently for each term in the sum over  $n$ . Under this assumption, the CEM predicts that the NRQCD production matrix elements are given by

$$\langle \mathcal{O}_n^H \rangle = \frac{1}{2\pi^2} F_H \int_0^{k_{\max}} k^2 dk \langle \mathcal{O}_n^{Q\bar{Q}}(k) \rangle. \quad (8)$$

The matrix elements on the right side of Eq. (8) can be computed in perturbation theory. Their dependences on  $\mathbf{k}$  are governed by the powers of the covariant derivative  $\mathbf{D}$  that appear in the factors  $\kappa_n$  and  $\kappa'_n$  of the operators. For the matrix element of leading order in  $v$  that corresponds to an operator of orbital-angular-momentum quantum number  $l$ , the matrix element is proportional to  $k^{2l}$ . Hence, the integral on the right side of Eq. (8) is proportional to  $k_{\max}^{2l+3}/(2l+3)$ . Since  $k_{\max}$  scales as  $v$ , the matrix element is suppressed as  $v^{2l}$  compared to the matrix element of an  $S$ -wave operator. Thus, the CEM implies a velocity-suppression pattern that is independent of the quarkonium state and depends only on the orbital-angular-momentum quantum number of the  $Q\bar{Q}$  pair. The suppression pattern for  $S$ -wave and  $P$ -wave matrix elements is shown in Table I. It should be contrasted with the intricate suppression pattern implied by NRQCD. We note that the relation (8) partially satisfies the constraints that are imposed by the velocity-scaling rules of NRQCD, in that there is an additional power of  $v^2$  for each unit of orbital angular momentum in the operator. However, powers of  $v$  that do not arise from the orbital angular momentum are not reproduced in the relation (8). This fact has been noted previously by Beneke [25].

Now let us state explicitly the relationships between the NRQCD matrix elements that are implied by the CEM relation (8). In the operator  $\mathcal{O}_n$ , let the subscript  $n$  represent the angular-momentum quantum numbers ( $s$ ,  $l$ , and  $j$ ) and the color state (singlet or octet). The standard forms of the operators are given in Ref. [1] for the first few  $S$ - and  $P$ -wave channels. The spin-triplet operators are normalized so that, if one makes the replacement  $\sigma_i \otimes \sigma_j \rightarrow \delta_{ij}(1 \otimes 1)$ , they become  $(2j+1)/(2l+1)$  times the corresponding spin-singlet operators. The color-octet operators are normalized so that, if one makes the replacement  $T^a \otimes T^a \rightarrow 1 \otimes 1$ , they become the corresponding color-singlet operators. The  $P$ -wave operators are normalized so that, if one makes the replacement  $(-\frac{i}{2}\overleftrightarrow{D}_i) \otimes (-\frac{i}{2}\overleftrightarrow{D}_j) \rightarrow \delta_{ij}(1 \otimes 1)$ , they become  $(2j+1)/(2s+1)$  times the corresponding  $S$ -wave operators. Given these normalization conventions, we find that the CEM relation (8) implies that the standard  $S$ -wave and  $P$ -wave NRQCD matrix elements are related by

$$\langle \mathcal{O}_n^H \rangle = \frac{3(2j+1)}{(2l+1)(2l+3)} C_n k_{\max}^{2l} \langle \mathcal{O}_1^H(^1S_0) \rangle, \quad (9)$$

where  $C_n = 1$  or  $(N_c^2 - 1)/(2N_c) = 4/3$  if  $\mathcal{O}_n^H$  is a color-singlet or color-octet operator, respectively. To be more specific, the CEM relation (8) implies that the  $S$ -wave matrix

elements are all related by simple group theory factors:

$$\langle \mathcal{O}_1^H(^3S_1) \rangle = 3 \langle \mathcal{O}_1^H(^1S_0) \rangle, \quad (10)$$

$$\langle \mathcal{O}_8^H(^1S_0) \rangle = \frac{4}{3} \langle \mathcal{O}_1^H(^1S_0) \rangle, \quad (11)$$

$$\langle \mathcal{O}_8^H(^3S_1) \rangle = 4 \langle \mathcal{O}_1^H(^1S_0) \rangle. \quad (12)$$

The  $P$ -wave matrix elements also include a factor  $k_{\max}^2$  from the integral over the relative momentum:

$$\langle \mathcal{O}_1^H(^1P_1) \rangle = \frac{3}{5} k_{\max}^2 \langle \mathcal{O}_1^H(^1S_0) \rangle, \quad (13)$$

$$\langle \mathcal{O}_1^H(^3P_J) \rangle = \frac{2J+1}{5} k_{\max}^2 \langle \mathcal{O}_1^H(^1S_0) \rangle, \quad (14)$$

$$\langle \mathcal{O}_8^H(^1P_1) \rangle = \frac{4}{5} k_{\max}^2 \langle \mathcal{O}_1^H(^1S_0) \rangle, \quad (15)$$

$$\langle \mathcal{O}_8^H(^3P_J) \rangle = \frac{4(2J+1)}{15} k_{\max}^2 \langle \mathcal{O}_1^H(^1S_0) \rangle. \quad (16)$$

#### IV. ANALYSIS OF $S$ -WAVE CHARMONIUM PRODUCTION

In the production of  $S$ -wave charmonium at the Tevatron with transverse momentum  $p_T > 5$  GeV, it is known phenomenologically that the most important NRQCD matrix elements for  $H = J/\psi$  or  $\psi(2S)$  are the color-octet matrix element  $\langle \mathcal{O}_8^H(^3S_1) \rangle$  and a specific linear combination of color-octet matrix elements  $\langle \mathcal{O}_8^H(^3P_0) \rangle$  and  $\langle \mathcal{O}_8^H(^1S_0) \rangle$ :

$$M_r^H = (r/m^2) \langle \mathcal{O}_8^H(^3P_0) \rangle + \langle \mathcal{O}_8^H(^1S_0) \rangle, \quad (17)$$

where  $r \approx 3$ . Let us examine the ratio of these matrix elements

$$R^H = \frac{M_r^H}{\langle \mathcal{O}_8^H(^3S_1) \rangle}, \quad (18)$$

where  $H$  stands for  $J/\psi$  or  $\psi(2S)$ . The relation (9) yields the CEM ratio

$$R_{\text{CEM}}^H = \frac{M_r^H}{\langle \mathcal{O}_8^H(^3S_1) \rangle} = \frac{r}{15} \frac{k_{\max}^2}{m^2} + \frac{1}{3}. \quad (19)$$

The velocity-scaling rules of NRQCD predict that all of the matrix elements in both the numerator and denominator of Eq. (18) scale as  $v^4$  relative to  $\langle \mathcal{O}_1^H(^3S_1) \rangle$ . Hence, the ratio in Eq. (18) is predicted to scale as  $v^0$ . Since  $k_{\max}$  scales as  $mv$ , the second term in the CEM ratio in Eq. (19) satisfies this scaling relation but the first term does not.

##### A. Analysis of Tevatron Data on $J/\psi$ Production

We now use the relation (9) to test the validity of the CEM in comparisons with data. In Table II, we show values of  $R^{J/\psi}$  for several different sets of NRQCD matrix elements that have been extracted, under varying assumptions, from the transverse-momentum distribution of  $J/\psi$ 's produced at the Tevatron. The matrix elements were

TABLE II: Values of  $R^{J/\psi}$ , as defined in Eq. (18), in the NRQCD factorization approach and in the CEM. The column labeled “ $R^{J/\psi}$ ” gives phenomenological values of  $R^{J/\psi}$  from various extractions of the NRQCD matrix elements from the CDF data [27]. The column labeled “Reference” gives the reference for each extraction, and the column labeled “PDF” gives the parton distribution that was used in the extraction. The headings “LO collinear factorization,” “parton-shower radiation,” and “ $k_T$  smearing” refer to the method that was used to compute the NRQCD factorization prediction. The column labeled “ $R_{\text{CEM}}^{J/\psi}$ ” gives the CEM ratios from Eq. (19) for the values of  $r$  and  $m_c$  that were used in the NRQCD extractions of  $R^{J/\psi}$ .

Reference	PDF	$R^{J/\psi}$	$R_{\text{CEM}}^{J/\psi}$	$r$	$m_c$ (GeV)	$\langle k_T \rangle$ (GeV)
LO collinear factorization						
[34]	MRS(D0) [35]	$10 \pm 4$	0.45	3	1.48	
[36]	CTEQ4L [37]	$4.1 \pm 1.2^{+3.6}_{-1.3}$	0.46	3.5	1.5	
	GRV-LO(94) [38]	$3.5 \pm 1.1^{+1.6}_{-0.9}$				
	MRS(R2) [39]	$7.8 \pm 1.9^{+8.0}_{-2.8}$				
[40]	MRST-LO(98) [32]	$20 \pm 4$	0.46	3.4	1.5	
	CTEQ5L [41]	$17 \pm 4$				
parton-shower radiation						
[42]	CTEQ2L [43]	$1.4 \pm 0.3$	0.45	3	1.48	
	MRS(D0) [35]	$1.9 \pm 0.6$				
	GRV-HO(94) [38]	$0.49 \pm 0.11$				
[44]	CTEQ4M [37]	$2.1 \pm 0.8$	0.44	3.5	1.55	
$k_T$ smearing						
[45]	CTEQ4M [37]	$5.7 \pm 1.6$	0.46	3.5	1.5	1.0
		$2.6 \pm 0.9$				1.5
[46]	MRS(D'_-) [35]	$6.3 \pm 1.7$	$\approx 0.44$	3	$\approx 1.5$	0.7
		$4.7 \pm 1.2$				1.0

taken from the compilation of Ref. [26]. We also show the CEM values  $R_{\text{CEM}}^{J/\psi}$ , taking  $k_{\text{max}}^2/m^2 = (m_D^2 - m_c^2)/m_c^2 \approx 0.54$ . Several sets of matrix elements were extracted by making use of NRQCD short-distance coefficients that were calculated at leading order in  $\alpha_s$  and under the assumption of standard collinear factorization. For these sets of matrix elements,  $R^{J/\psi}$  is much larger than  $R_{\text{CEM}}^{J/\psi}$ . Multiple gluon radiation, as modeled by parton-shower Monte Carlo, tends to increase the partonic cross section more at smaller values of  $p_T$  than at larger values of  $p_T$ . Since the contribution of  $\langle \mathcal{O}_8^{J/\psi}(^3S_1) \rangle$  dominates that of  $M_r^{J/\psi}$  at large  $p_T$ , while the contribution of  $M_r^{J/\psi}$  is the more important one at small  $p_T$ , the effect of parton showering is to decrease the size of  $R^{J/\psi}$ . Hence, the addition of parton showering to the leading-order calculation of the NRQCD short-distance coefficients brings the ratio  $R^{J/\psi}$  for the extracted values of the matrix elements into better agreement with the  $R_{\text{CEM}}^{J/\psi}$ . However, the extraction that is based on the more recent CTEQ(4M) parton distributions is still in significant disagreement with  $R_{\text{CEM}}^{J/\psi}$ . Surprisingly,  $k_T$  smearing does not decrease the size of  $R^{J/\psi}$  as much as parton showering, and there is a substantial disagreement between

$R_{\text{CEM}}^{J/\psi}$  and the values of  $R^{J/\psi}$  that are obtained by using  $k_T$  smearing.

Now let us compare the predictions of the CEM and NRQCD factorization directly with the CDF data [27]. The CEM predictions are from a calculation by Vogt [28] that makes use of the order- $\alpha_s^3$  cross section for production of a  $Q\bar{Q}$  pair [29]. Details of this calculation are given in Ref. [4]. The CEM factors  $F_H$  in Eq. (4) were fixed by comparison with fixed-target data. The NRQCD predictions were generated from modified versions of computer codes created by Maltoni, Mangano, and Petrelli [30]. The codes compute the order- $\alpha_s^3$  quarkonium production cross sections [31] and the standard DGLAP evolution of the fragmentation contribution to the evolution of a  $Q\bar{Q}$  pair in a  $^3S_1$  color-octet state into a quarkonium. This fragmentation contribution is the dominant contribution at large  $p_T$ .

Plots of (data – theory)/theory are shown for the CEM and NRQCD factorization predictions in Fig. 1. The predictions are based on the MRST98 HO parton distributions [32] and the GRV98 HO [33] parton distributions. There is a substantial disagreement between the CEM predictions and the data. The normalization of the CEM prediction is too small, and the slope is relatively too positive. This discrepancy in the slope is consistent with the fact that the CEM relation (19) over-estimates the size of  $\langle \mathcal{O}_8^{J/\psi}(^3S_1) \rangle$  relative to  $M_r^{J/\psi}$ . The NRQCD factorization prediction is in much better agreement with the data than the CEM prediction. Even if one were to adjust the normalization of the CEM predictions to improve the fit, the NRQCD factorization fit would still be superior, as it is much better able to account for the slope of the data.

A simple phenomenological model for the effects of multiple gluon emission on the theoretical predictions is  $k_T$  smearing. In  $k_T$  smearing, the colliding partons are given Gaussian distributions in the intrinsic transverse momentum, with a width that is treated as a phenomenological parameter. A particular version of this model that has been used in comparing the CEM predictions with the experimental data [4, 28] attempts to account for multiple gluon emission from the two initial-state partons by adding two transverse-momentum “kicks” to the quarkonium momentum. The direction of each momentum kick is symmetrically distributed over the  $4\pi$  solid angle, and the magnitude  $k_T$  of each momentum kick is distributed as

$$g(k_T) = \frac{1}{\pi \langle k_T^2 \rangle} \exp(-k_T^2 / \langle k_T^2 \rangle), \quad (20)$$

where  $\langle k_T^2 \rangle$  is a phenomenological parameter. In the case of the CEM predictions with  $k_T$  smearing,  $\langle k_T^2 \rangle$  has been tuned to the value  $\langle k_T^2 \rangle = 2.5 \text{ GeV}^2$  in order to obtain the best fit to the CDF  $J/\psi$  data [4, 28]. This same value was also used in making CEM predictions for  $\psi(2S)$  and  $\chi_c$  production. For purposes of comparison, we also take  $\langle k_T^2 \rangle = 2.5 \text{ GeV}^2$  when we apply  $k_T$  smearing to the NRQCD factorization predictions for charmonium production.

Plots of (data – theory)/theory for the CEM and NRQCD factorization predictions with  $k_T$  smearing are shown in Fig. 2. The  $k_T$ -smearing procedure substantially improves both the slope and normalization of the CEM fits to the data and slightly worsens the NRQCD factorization fits to the data.<sup>3</sup> The improvement of the slopes of the CEM predictions with  $k_T$  smearing is to be expected since, generally, the effect of  $k_T$  smearing is to increase the

---

<sup>3</sup> The effects of  $k_T$  smearing on predictions for  $J/\psi$  production cross sections at the Tevatron have also been studied by Sridhar, Martin, and Stirling [46] and Petrelli [45]. These studies made use of somewhat smaller values of  $\langle k_T^2 \rangle$  than in the present work. They also concluded that the quality of the NRQCD factorization fits to the CDF data is little affected by  $k_T$  smearing.

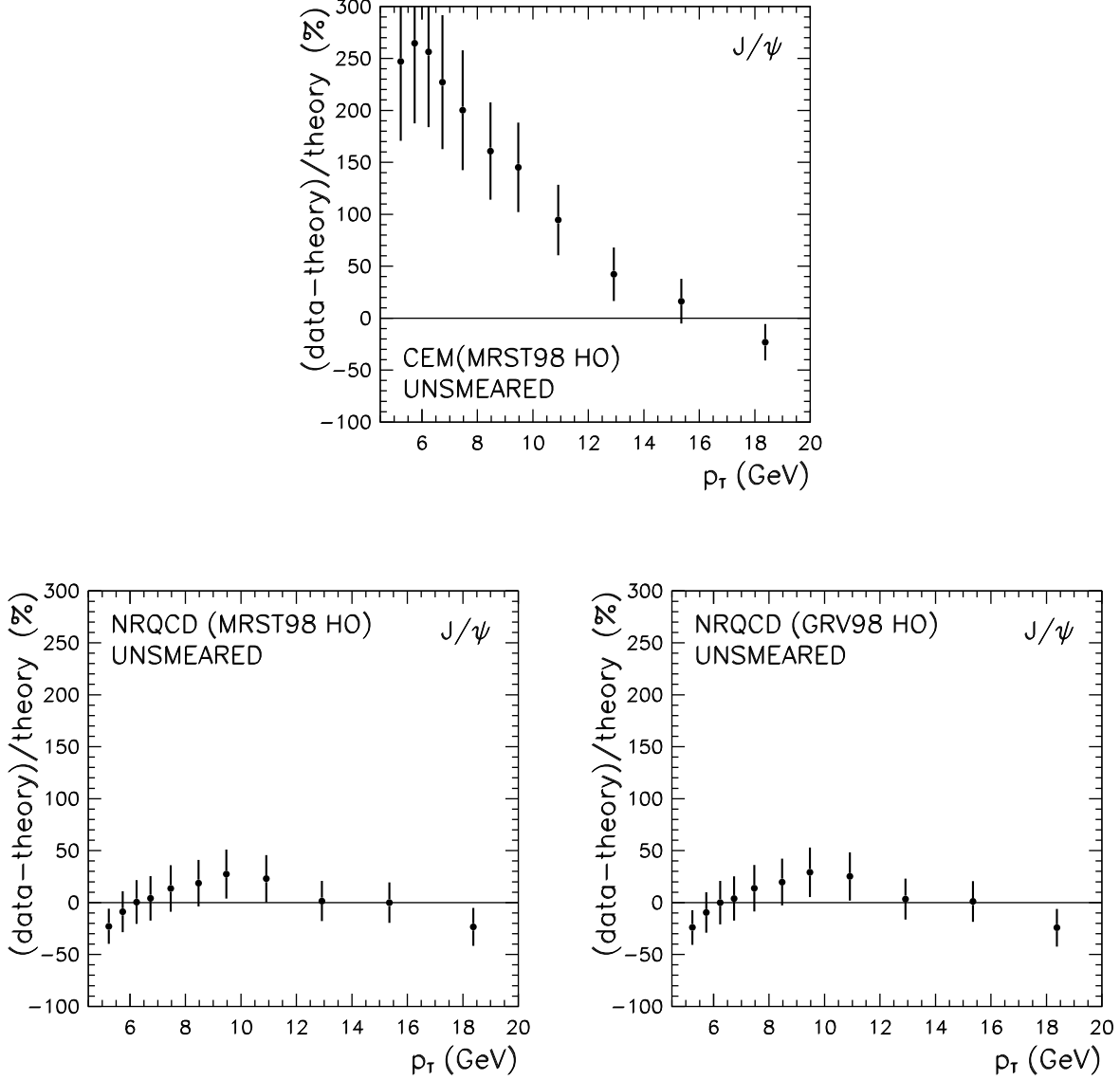


FIG. 1:  $J/\psi$  production:  $(\text{data} - \text{theory}) / \text{theory}$ . The data are from the measurements of the CDF collaboration [27]. The upper figure is for the CEM prediction, using the MRST98 HO parton distributions [32]. The lower left-hand and right-hand figures are for the NRQCD factorization predictions, using the MRST98 HO [32] and GRV98 HO [33] parton distributions, respectively.

cross section considerably at moderate values of  $p_T$  and increase the cross section by a smaller amount at high  $p_T$ . Nevertheless, the  $k_T$ -smeared CEM fits are still considerably worse than the  $k_T$ -smeared NRQCD factorization fits. Even for the  $k_T$ -smeared CEM predictions, the slopes are too positive relative to the data. This is consistent with the fact that the CEM relation (19) over-estimates the size of  $\langle \mathcal{O}_8^{J/\psi}(^3S_1) \rangle$  relative to  $M_r^{J/\psi}$ , even for  $k_T$ -smeared extractions of the matrix elements.

A compilation of values of matrix elements, values of  $R^{J/\psi}$ , and chi-squared per degree of freedom ( $\chi^2/\text{d.o.f.}$ ) from the NRQCD factorization fits and CEM fits to the  $J/\psi$  data is

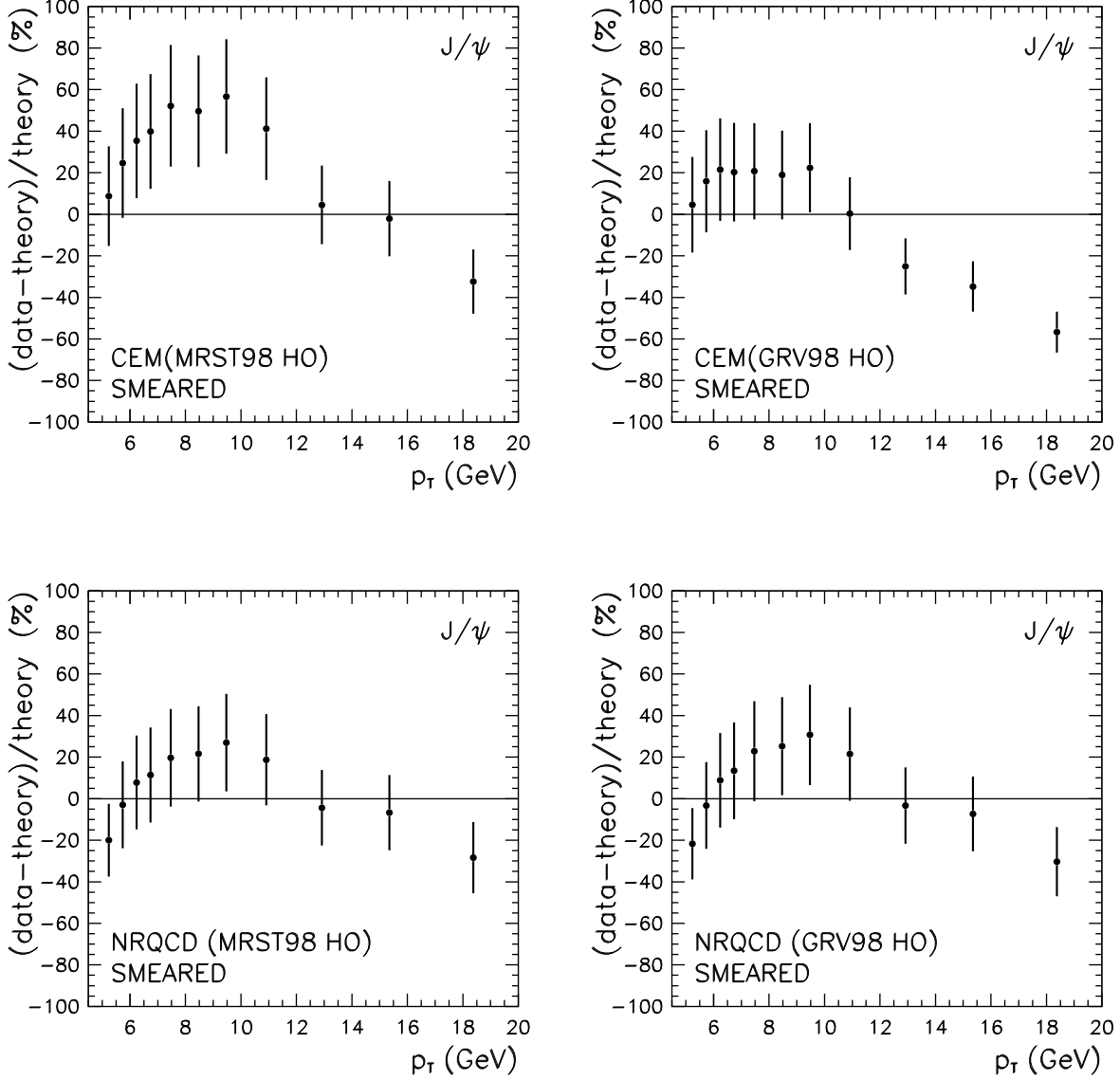


FIG. 2:  $J/\psi$  production:  $(\text{data} - \text{theory})/\text{theory}$ , with  $k_T$  smearing of the theory, as described in the text. The data are from the measurements of the CDF collaboration [27]. The upper figures are for the CEM predictions and the lower figures are for the NRQCD factorization predictions. The theoretical predictions for the left-hand and right-hand figures are based on the MRST98 HO [32] and the GRV98 HO [33] parton distributions, respectively.

given in Table III. In the NRQCD factorization fits, the degrees of freedom are reduced by two, owing to the two NRQCD matrix elements that are varied in the fits. The unsmeared CEM fits have no free parameters, as the overall normalization is fixed by comparison with the fixed-target data. The smeared CEM fits to the  $J/\psi$  data have one free parameter,  $\langle k_T^2 \rangle$ , which is then held constant in fits to the  $\psi(2S)$  and  $\chi_c$  data. The values of  $R^{J/\psi}$  in Table III are much greater than  $R_{\text{CEM}}^{J/\psi} = 0.46$  in the fits without  $k_T$  smearing and somewhat greater than  $R_{\text{CEM}}^{J/\psi}$  in the fits with  $k_T$  smearing. The relative values of  $R^{J/\psi}$  and  $R_{\text{CEM}}^{J/\psi}$  are

TABLE III: Values of matrix elements,  $R^{J/\psi}$ , and  $\chi^2/\text{d.o.f.}$  from the NRQCD factorization and CEM fits to the  $J/\psi$  data. In the NRQCD factorization fits, we set  $\langle \mathcal{O}_1^{J/\psi}(^3S_1) \rangle = 1.16 \text{ GeV}^3$  and give the fitted values of  $\langle \mathcal{O}_8^{J/\psi}(^3S_1) \rangle$  and  $M_{3.5}^{J/\psi}$ .

PDF	$\langle \mathcal{O}_8^{J/\psi}(^3S_1) \rangle$ ( $\text{GeV}^3 \times 10^{-2}$ )	$M_{3.5}^{J/\psi}$ ( $\text{GeV}^3 \times 10^{-2}$ )	$R^{J/\psi}$	$\chi^2/\text{d.o.f.}$
NRQCD Factorization				
MRST98 HO	$1.04 \pm 0.22$	$14.8 \pm 2.1$	$14.2 \pm 3.6$	$7.17/(11-2)=0.80$
GRV98 HO	$1.07 \pm 0.23$	$17.9 \pm 2.4$	$16.7 \pm 4.2$	$7.99/(11-2)=0.89$
MRST98 HO (smeared)	$1.34 \pm 0.13$	$1.30 \pm 0.35$	$0.97 \pm 0.28$	$8.28/(11-2)=0.92$
GRV98 HO (smeared)	$1.46 \pm 0.14$	$1.57 \pm 0.39$	$1.07 \pm 0.29$	$10.19/(11-2)=1.13$
Color-Evaporation Model				
MRST98 HO				$95.12/11=8.65$
MRST98 HO (smeared)				$22.82/(11-1)=2.82$
GRV98 HO (smeared)				$49.29/(11-1)=4.93$

consistent with the large discrepancy between the slopes of the NRQCD factorization and CEM fits without  $k_T$  smearing and the smaller discrepancy between the slopes of the NRQCD factorization and CEM fits with  $k_T$  smearing.

## B. Analysis of Tevatron Data on $\psi(2S)$ Production

Next let us examine the case of  $\psi(2S)$  production. In Table IV we show values of  $R^{\psi(2S)}$  that were obtained from several different sets of NRQCD matrix elements that have been extracted from the transverse-momentum distribution of  $\psi(2S)$ 's produced at the Tevatron. Again, the matrix elements were taken from the compilation of Ref. [26]. We also show the CEM values  $R_{\text{CEM}}^{\psi(2S)}$  in Table IV. As in the analysis of the  $J/\psi$  data, the values of  $R^{\psi(2S)}$  lie substantially above  $R_{\text{CEM}}^{\psi(2S)}$ , except in the case of the matrix elements that were extracted by making use of the GRV-HO(94) parton distributions and parton-shower radiation in computing the NRQCD factorization predictions.

Plots of  $(\text{data} - \text{theory})/\text{theory}$  for the CEM and NRQCD factorization predictions for  $\psi(2S)$  production are shown in Fig. 3. Owing to their larger error bars, the  $\psi(2S)$  data have less discriminating power than the  $J/\psi$  data. Nevertheless, it can be seen that the CEM predictions for  $\psi(2S)$  production fit the data poorly, while the NRQCD factorization predictions fit the data almost too well. (It should be remembered that the error bars on the CDF data reflect both systematic and statistical uncertainties.) As in the case of  $J/\psi$  production, the CEM predictions have an overall normalization that is too low and a slope that is too positive. Again, the discrepancy in the slope is expected from the fact that the CEM relation (19) over-estimates the size of  $\langle \mathcal{O}_8^{\psi(2S)}(^3S_1) \rangle$  relative to  $M_r^{\psi(2S)}$ . Even if the normalizations of the CEM prediction were adjusted to fit the data, the overall fit would be poorer than those of the NRQCD factorization predictions.

Plots of  $(\text{data} - \text{theory})/\text{theory}$  for the  $k_T$ -smeared CEM and NRQCD factorization predictions for  $\psi(2S)$  production are shown in Fig. 4. The effect of  $k_T$  smearing is to

TABLE IV: Values of  $R^{\psi(2S)}$ , as defined in Eq. (18), in the NRQCD factorization approach and in the CEM. As in Table II, but for  $\psi(2S)$ .

Reference	PDF	$R^{\psi(2S)}$	$R_{\text{CEM}}^{\psi(2S)}$	$r$	$m_c$ (GeV)
LO collinear factorization					
[34]	MRS(D0) [35]	$3.8 \pm 1.5$	0.45	3	1.48
[36]	CTEQ4L [37]	$4.1 \pm 1.5^{+3.4}_{-1.3}$	0.46	3.5	1.5
	GRV-LO(94) [38]	$3.5 \pm 1.3^{+1.6}_{-0.9}$			
	MRS(R2) [39]	$7.8 \pm 2.3^{+8.3}_{-2.8}$			
[40]	MRST-LO(98) [32]	$3.1 \pm 1.4$	0.46	3.5	1.5
	CTEQ5L [41]	$2.1 \pm 1.1$			
parton-shower radiation					
[42, 47]	CTEQ2L [43]	$2.4 \pm 0.8$	0.45	3	1.48
	MRS(D0) [35]	$2.5 \pm 0.9$			
	GRV-HO(94) [38]	$0.28 \pm 0.35$			

improve both the CEM and NRQCD factorization fits. The CEM fits are improved in both normalization and slope. Even so, the  $k_T$ -smeared CEM fits are substantially worse than the  $k_T$ -smeared NRQCD factorization fits. The CEM fits would remain inferior to the NRQCD factorization fits even if their normalizations were adjusted to improve the fits. The matrix elements and  $\chi^2/\text{d.o.f.}$  from the NRQCD factorization fits and CEM fits to the  $\psi(2S)$  data are given in Table V. The values of  $R^{\psi(2S)}$  in Table V are much greater than  $R_{\text{CEM}}^{\psi(2S)} = 0.46$  in the fits without  $k_T$  smearing and consistent with  $R_{\text{CEM}}^{\psi(2S)}$  (and with zero) in the fits with  $k_T$  smearing. The relative values of  $R^{\psi(2S)}$  and  $R_{\text{CEM}}^{\psi(2S)}$  are consistent with the large discrepancy between the slopes of the NRQCD factorization and CEM fits without  $k_T$  smearing and the approximate agreement of the slopes of the NRQCD factorization and CEM fits with  $k_T$  smearing.

## V. ANALYSIS OF $P$ -WAVE CHARMONIUM PRODUCTION

Now let us turn to the case of production of the  $P$ -wave charmonium states  $\chi_{cJ}$  ( $J = 0, 1, 2$ ) at the Tevatron at transverse momenta  $p_T > 5$  GeV. It is known phenomenologically that the most important NRQCD matrix elements are the color-singlet matrix elements  $\langle \mathcal{O}_1^{\chi_{cJ}}(^3P_J) \rangle$  and the color-octet matrix elements  $\langle \mathcal{O}_8^{\chi_{cJ}}(^3S_1) \rangle$ . The three color-singlet matrix elements can be expressed in terms of  $\langle \mathcal{O}_1^{\chi_{c0}}(^3P_0) \rangle$ , and the three color-octet matrix elements can be expressed in terms of  $\langle \mathcal{O}_8^{\chi_{c0}}(^3S_1) \rangle$  by making use of the heavy-quark spin-symmetry relations

$$\langle \mathcal{O}_{1,8}^{\chi_{cJ}}(^3P_J) \rangle = (2J + 1) \langle \mathcal{O}_{1,8}^{\chi_{c0}}(^3P_0) \rangle, \quad (21)$$

which hold up to corrections of order  $v^2$ . Therefore, we define a ratio

$$R^{\chi_c} = \frac{\langle \mathcal{O}_8^{\chi_{c0}}(^3S_1) \rangle}{\langle \mathcal{O}_1^{\chi_{c0}}(^3P_0) \rangle / m^2}. \quad (22)$$

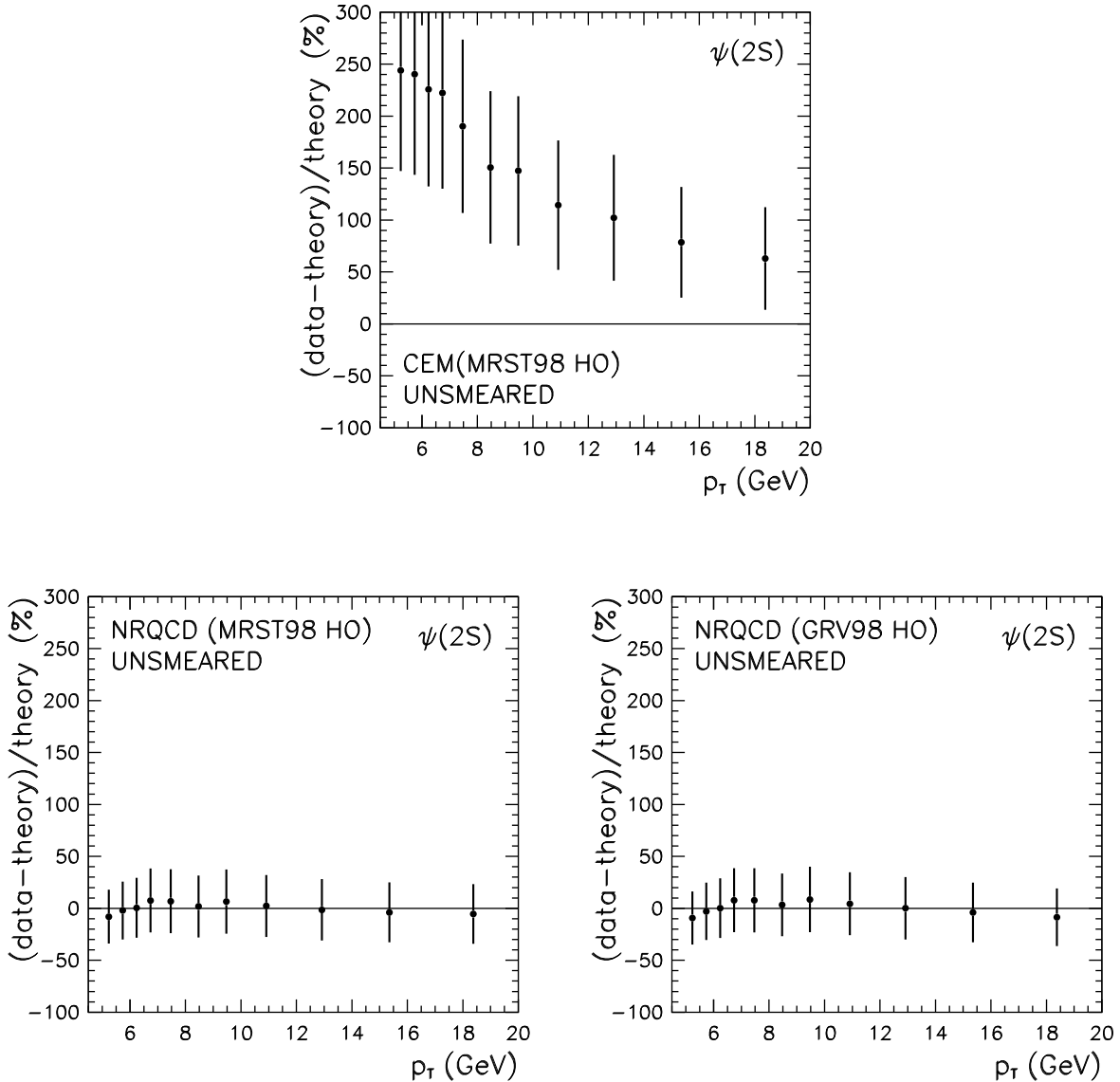


FIG. 3:  $\psi(2S)$  production:  $(\text{data} - \text{theory})/\text{theory}$ . As in Fig. 1, but for  $\psi(2S)$ .

The relation (9) yields the CEM prediction

$$R_{\text{CEM}}^{x_c} = 15C_F \frac{m^2}{k_{\text{max}}^2}. \quad (23)$$

The velocity-scaling rules of NRQCD predict that the ratio  $R^{x_c}$  in Eq. (22) scales as  $v^0$ . In contrast, we see that the CEM prediction in Eq. (23) scales as  $v^{-2}$ . Furthermore, with the standard normalization of the NRQCD matrix elements in Ref. [1], the color factor in  $R^{x_c}$  is estimated [31] to be  $1/(2N_c) = 1/6$ , while the CEM prediction is that the color factor in  $R^{x_c}$  is  $C_F = 4/3$ . Both the discrepancy in the velocity scaling and the discrepancy in the color factor have the effect of increasing the size of the CEM prediction relative to the expectation from NRQCD.

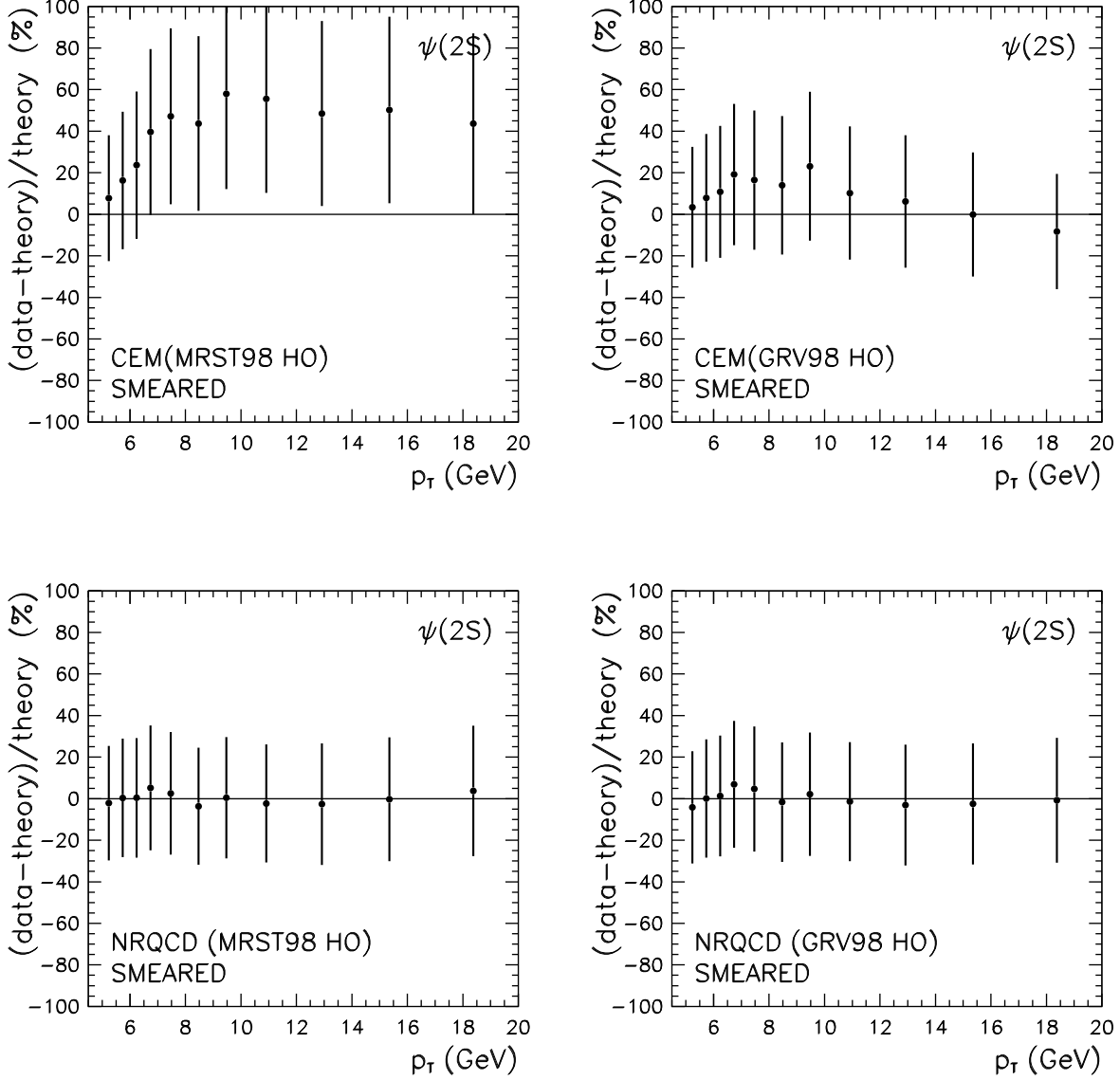


FIG. 4:  $\psi(2S)$  production:  $(\text{data} - \text{theory})/\text{theory}$ , with  $k_T$  smearing of the theory, as described in the text. As in Fig. 2, but for  $\psi(2S)$ .

In Table VI we show values of  $R^{Xc}$  that were obtained from several different sets of NRQCD matrix elements that have been extracted from the transverse-momentum distribution of  $J/\psi$ 's produced at the Tevatron. Again, the matrix elements were taken from the compilation of Ref. [26]. The values of  $R^{Xc}$  in Table VI are reasonably close to the value  $R^{Xc} \approx v^0/(2N_c) \approx 0.17$  that one would expect on the basis of the velocity-scaling rules and the estimate of the color factor. Table VI also contains the CEM values  $R_{\text{CEM}}^{Xc}$ . As expected, they are much larger than the values of  $R^{Xc}$  that follow from the data.<sup>4</sup> Consequently, we expect the CEM to predict a cross section that is relatively too large at high  $p_T$ , where the

<sup>4</sup> Because the CEM prediction scales incorrectly with  $v$ , we expect the disagreement between the CEM ratio

TABLE V: Values of matrix elements,  $R^{\psi(2S)}$ , and  $\chi^2/\text{d.o.f.}$  from the NRQCD factorization and CEM fits to the  $\psi(2S)$  data. In the NRQCD factorization fits, we set  $\langle \mathcal{O}_1^{\psi(2S)}(^3S_1) \rangle = 0.76 \text{ GeV}^3$  and give the fitted values of  $\langle \mathcal{O}_8^{\psi(2S)}(^3S_1) \rangle$  and  $M_{3,5}^{\psi(2S)}$ .

PDF	$\langle \mathcal{O}_8^{\psi(2S)}(^3S_1) \rangle$ ( $\text{GeV}^3 \times 10^{-3}$ )	$M_{3,5}^{\psi(2S)}$ ( $\text{GeV}^3 \times 10^{-4}$ )	$R^{\psi(2S)}$	$\chi^2/\text{d.o.f.}$
NRQCD Factorization				
MRST98 HO	$2.38 \pm 0.47$	$71.5 \pm 33.1$	$3.00 \pm 1.51$	$0.32/(11-2)=0.04$
GRV98 HO	$2.56 \pm 0.52$	$92.0 \pm 38.0$	$3.58 \pm 1.65$	$0.49/(11-2)=0.05$
MRST98 HO (smeared)	$2.09 \pm 0.27$	$-8.09 \pm 5.30$	$-3.87 \pm 2.58$	$0.09/(11-2)=0.01$
GRV98 HO (smeared)	$2.31 \pm 0.30$	$-7.14 \pm 5.85$	$-3.09 \pm 2.58$	$0.13/(11-2)=0.01$
Color-Evaporation Model				
MRST98 HO				$47.79/11=3.44$
MRST98 HO (smeared)				$10.60/11=0.96$
GRV98 HO (smeared)				$1.58/11=0.14$

TABLE VI: Values of  $R^{\chi_c}$ , as defined in Eq. (22), in the NRQCD factorization approach and in the CEM. As in Table II, except for  $\chi_c$ . The column labeled “ $R_{\text{CEM}}^{\chi_c}$ ” gives the CEM ratios from Eq. (23) for the values of  $m_c$  that were used in the NRQCD extractions of  $R^{\chi_c}$ .

Reference	PDF	$R^{\chi_c}$	$R_{\text{CEM}}^{\chi_c}$	$m_c$ (GeV)
LO collinear factorization				
[34]	MRS(D0) [35]	$(6.6 \pm 0.8) \times 10^{-2}$	35	1.48
[44]	CTEQ4L [37]	$(0.71 \pm 0.21) \times 10^{-2}$	45	1.55
[40]	MRST-LO(98) [32]	$(5.8 \pm 1.1) \times 10^{-2}$	37	1.5
	CTEQ5L [41]	$(4.7 \pm 0.8) \times 10^{-2}$		

contribution from  $\langle \mathcal{O}_8^{\chi_{c0}}(^3S_1) \rangle$  dominates, in comparison with the cross section at low  $p_T$ , where the contribution from  $\langle \mathcal{O}_1^{\chi_{c0}}(^3P_0) \rangle$  dominates.

Plots of (data – theory)/theory for the CEM and NRQCD factorization predictions for  $\chi_c$  production are shown in Fig. 5. In the NRQCD factorization fits, we have fixed the value of  $\langle \mathcal{O}_1^{\chi_{c0}}(^3P_0) \rangle$  to be  $0.09 \text{ GeV}^3$ . This value is approximately equal to the value of the corresponding decay matrix element that has been obtained in a global fit to the existing data for inclusive decays of  $\chi_c$  states [48]. Color-singlet decay and production matrix elements are simply related, up to corrections of order  $v^4$  [1]. Both the CEM and NRQCD factorization predictions have normalizations that are too small and slopes that are too positive relative to the data. Both fits show substantial disagreements with the slope of the data. However, the discrepancies are considerably greater in the CEM fit than in the NRQCD factorization fits. The larger discrepancy in slope in the CEM fit is in accordance with our discussion of

---

and the value extracted from the data to be even more dramatic for  $R^{\chi_b}$  than for  $R^{\chi_c}$ . For  $m_b = 4.7 \text{ GeV}$  and  $m_B = 5.28 \text{ GeV}$ , the CEM ratio predicted by Eq. (23) is  $R_{\text{CEM}}^{\chi_b} \approx 76$ , while the expectation from NRQCD is that  $R^{\chi_b}$  should be comparable to  $R^{\chi_c}$ .

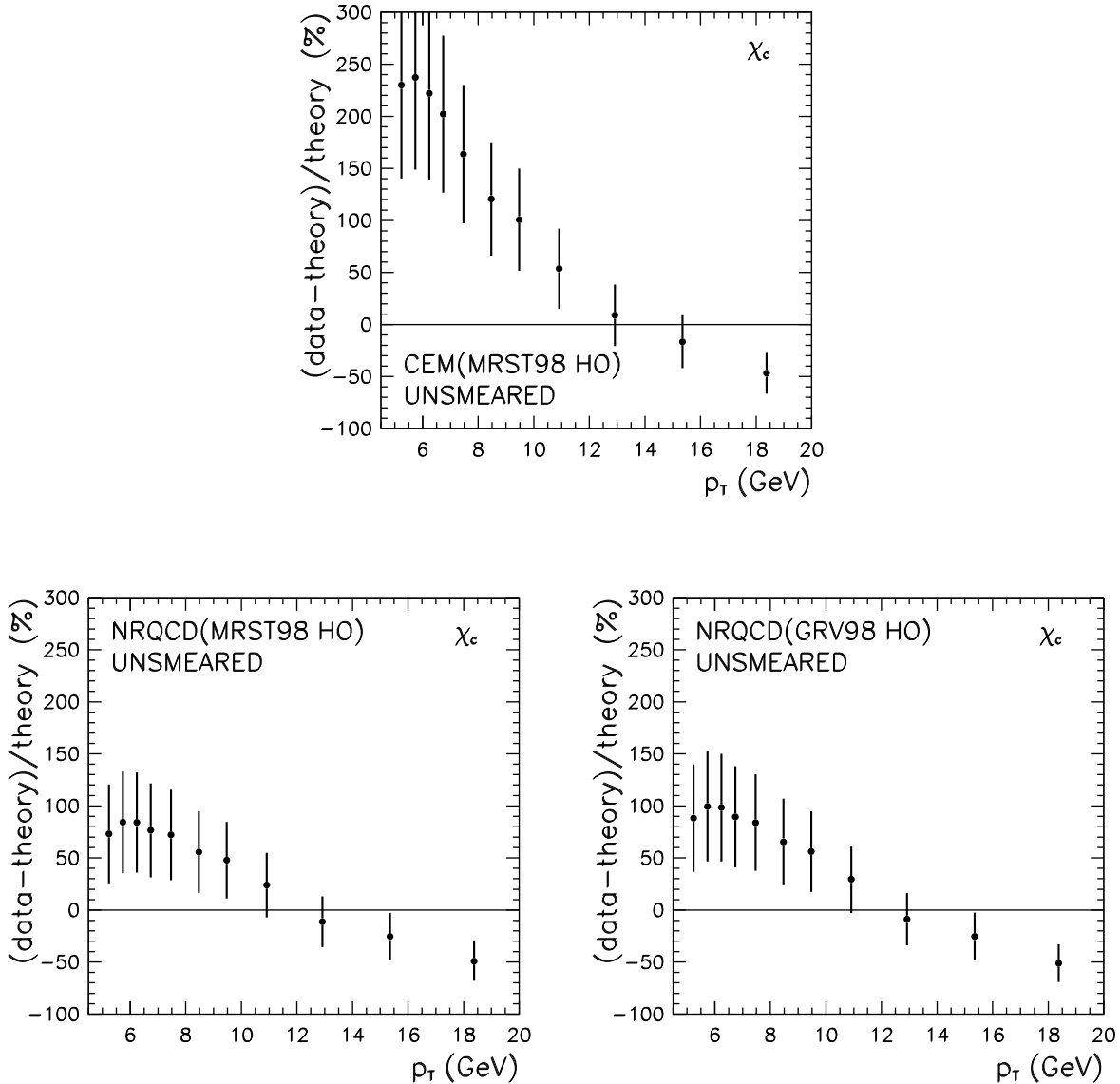


FIG. 5:  $\chi_c$  production:  $(\text{data} - \text{theory})/\text{theory}$ . As in Fig. 1, but for  $\chi_c$ .

$R^{\chi_c}$  above.

Plots of  $(\text{data} - \text{theory})/\text{theory}$  for the  $k_T$ -smeared CEM and NRQCD factorization predictions for  $\chi_c$  production are shown in Fig. 6. The effect of  $k_T$  smearing is to improve both the CEM and NRQCD factorization fits. However, the CEM prediction is still substantially too large at high  $p_T$ , and the NRQCD factorization fit is now too large at low  $p_T$ . The NRQCD factorization fit is still superior to the CEM fit and agrees reasonably well with the data.

A compilation of values of matrix elements, values of  $R^{\chi_c}$ , and  $\chi^2/\text{d.o.f.}$  from the NRQCD factorization and CEM fits to the  $\chi_c$  data are given in Table VII. The values of  $R^{\chi_c}$  in Table VII are much less than  $R_{\text{CEM}}^{\chi_c} = 37$ . The relative values of  $R^{\chi_c}$  and  $R_{\text{CEM}}^{\chi_c}$  are consistent with the large discrepancies between the slopes of the NRQCD factorization and CEM

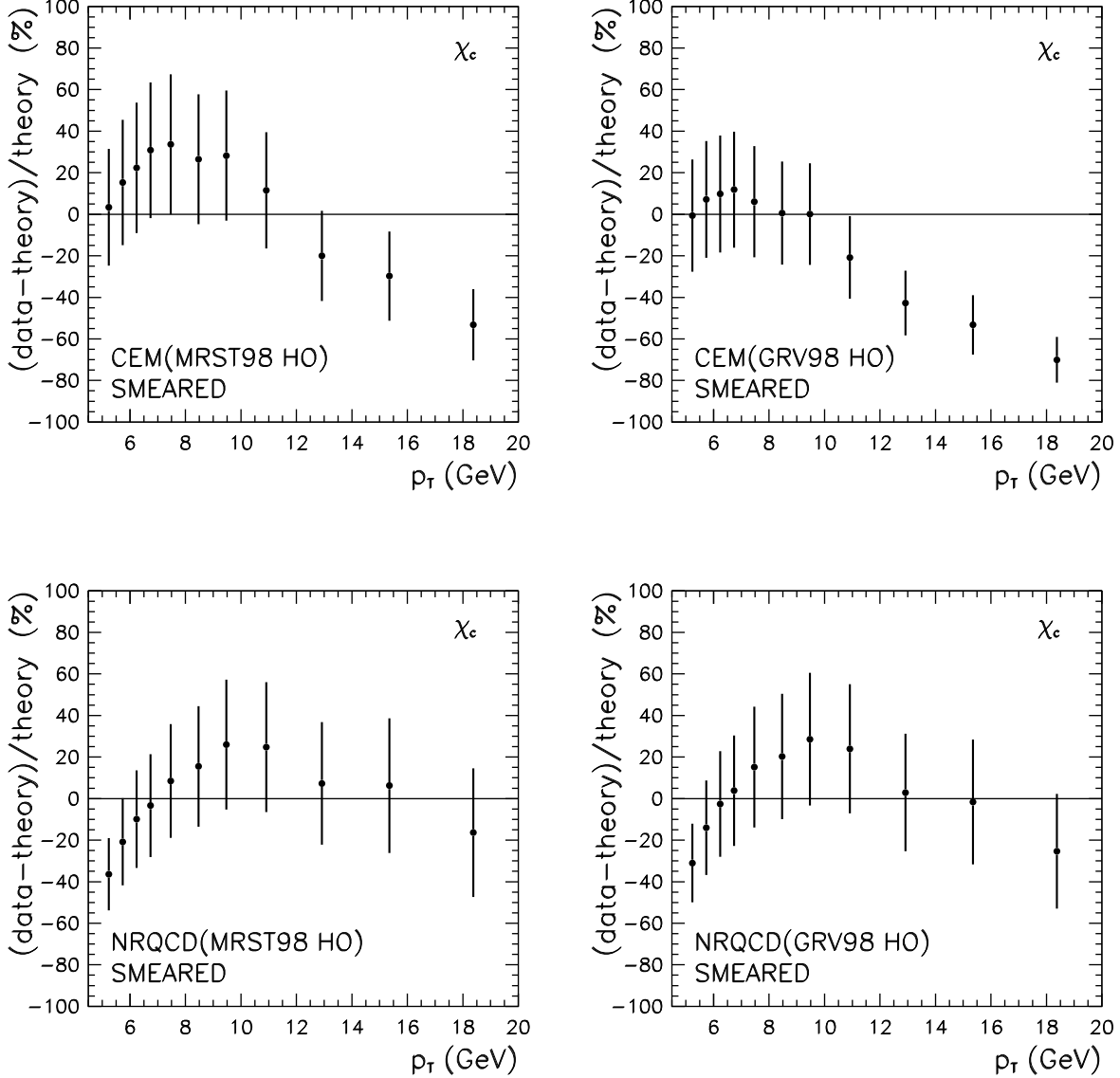


FIG. 6:  $\chi_c$  production:  $(\text{data} - \text{theory})/\text{theory}$ , with  $k_T$  smearing of the theory, as described in the text. As in Fig. 2, but for  $\chi_c$ .

fits. As we have mentioned, in fitting the predictions of NRQCD factorization to the CDF data, we have fixed the value of  $\langle \mathcal{O}_1^{\chi_{c0}}({}^3P_0) \rangle$  to be  $0.09 \text{ GeV}^3$ . Alternatively, we can treat  $\langle \mathcal{O}_1^{\chi_{c0}}({}^3P_0) \rangle$  as a free parameter in the fits. The results of this exercise are shown in the lower rows of the NRQCD factorization part of Table VII. In the fits without  $k_T$  smearing, the values of  $\langle \mathcal{O}_1^{\chi_{c0}}({}^3P_0) \rangle$  that are obtained are about a factor of four larger than the phenomenological value of the corresponding decay matrix element [48]. Even given the large theoretical uncertainties in the determination of the decay matrix element, this discrepancy is unacceptably large. Thus, we conclude that the disagreement of the constrained, unsmeared NRQCD factorization prediction with the  $\chi_c$  data cannot be ameliorated by treating  $\langle \mathcal{O}_1^{\chi_{c0}}({}^3P_0) \rangle$  as a free parameter. On the other hand, the values of  $\langle \mathcal{O}_1^{\chi_{c0}}({}^3P_0) \rangle$  that

TABLE VII: Values of matrix elements,  $R^{\chi_c}$ , and  $\chi^2/\text{d.o.f.}$  from the NRQCD factorization and CEM fits to the  $\chi_c$  data. In the NRQCD factorization fits, the upper sets of parameters are for fits in which  $\langle \mathcal{O}_1^{\chi_{c0}}(^3P_0) \rangle$  is fixed, as described in the text, while the lower sets of parameters are for fits in which  $\langle \mathcal{O}_1^{\chi_{c0}}(^3P_0) \rangle$  is varied.

PDF	$\langle \mathcal{O}_1^{\chi_{c0}}(^3P_0) \rangle$ ( $\text{GeV}^5 \times 10^{-2}$ )	$\langle \mathcal{O}_8^{\chi_{c0}}(^3S_1) \rangle$ ( $\text{GeV}^3 \times 10^{-3}$ )	$R^{\chi_c}$ ( $10^{-2}$ )	$\chi^2/\text{d.o.f.}$
NRQCD Factorization				
MRST98 HO	9.0 (input)	$3.50 \pm 0.40$	$8.75 \pm 1.00$	$26.6/(11-1)=2.66$
GRV98 HO	9.0 (input)	$3.86 \pm 0.43$	$9.65 \pm 1.08$	$31.5/(11-1)=3.15$
MRST98 HO (smeared)	9.0 (input)	$1.73 \pm 0.29$	$4.33 \pm 0.73$	$7.6/(11-1)=0.76$
GRV98 HO (smeared)	9.0 (input)	$2.12 \pm 0.32$	$5.30 \pm 0.80$	$6.1/(11-1)=0.61$
MRST98 HO	$39.3 \pm 6.2$	$1.29 \pm 0.60$	$0.74 \pm 0.36$	$3.00/(11-2)=0.33$
GRV98 HO	$47.0 \pm 7.1$	$1.27 \pm 0.65$	$0.61 \pm 0.32$	$3.24/(11-2)=0.36$
MRST98 HO (smeared)	$6.36 \pm 1.46$	$2.18 \pm 0.38$	$7.71 \pm 2.22$	$4.34/(11-2)=0.48$
GRV98 HO (smeared)	$7.50 \pm 1.63$	$2.37 \pm 0.41$	$7.11 \pm 1.37$	$5.23/(11-2)=0.58$
Color-Evaporation Model				
MRST98 HO				$51.60/11=4.69$
MRST98 HO (smeared)				$16.73/11=1.52$
GRV98 HO (smeared)				$63.57/11=5.78$

are obtained in the fits with  $k_T$  smearing are in good agreement with the phenomenological value of corresponding decay matrix element. These results, suggest that, if the NRQCD factorization picture is valid, then multiple gluon emission (as modeled by  $k_T$  smearing) is essential in obtaining the correct shape of the cross section as a function of  $p_T$ .

## VI. CONCLUSIONS

In this paper, we have compared the CEM and NRQCD factorization approaches to inclusive quarkonium production. As we have mentioned, the predictions of the CEM are at odds with a number of experimental observations. These include the different fractions of  $J/\psi$ 's from  $\chi_c$  decays that occur in  $B$  decays and in prompt production at the Tevatron, the nonzero polarization of  $J/\psi$ 's in  $e^+e^-$  annihilation at the  $B$  factories, the nonzero polarization of  $\Upsilon(2S)$  and  $\Upsilon(3S)$  in a fixed-target experiment, and the deviation from  $3/5$  of the ratio of the prompt-production cross sections for  $\chi_{c1}$  and  $\chi_{c2}$  at the Tevatron. Nevertheless, one might hope that the CEM would still be useful for predicting rates of inclusive quarkonium production at large  $p_T$ .

By making use of the NRQCD factorization expressions for the quarkonium production cross section and for the perturbative  $Q\bar{Q}$  production cross section, we have translated the CEM assumptions into predictions for the ratios of NRQCD production matrix elements. A comparison of the CEM ratios with the phenomenological ratios that have been extracted from the CDF data indicates that the CEM predicts a ratio  $M_r^H/\langle \mathcal{O}_8^H(^3S_1) \rangle$  that is too small in  $J/\psi$  and  $\psi(2S)$  production and a ratio  $\langle \mathcal{O}_8^{\chi_{c0}}(^3S_1) \rangle/\langle \mathcal{O}_1^{\chi_{c0}}(^3P_0) \rangle$  that is too large in  $\chi_c$  production. Both of these predictions of the CEM would be expected to lead to

cross sections that have too positive a slope, as a function of  $p_T$ , relative to the data. This expectation is borne out by comparisons of the CEM with the CDF data for  $J/\psi$ ,  $\psi(2S)$ , and  $\chi_c$  production. In contrast, the NRQCD factorization fits to the data do not show such a trend, except in the case of  $\chi_c$  production, in which there is a substantial disagreement between the NRQCD prediction and the shape of the data. The NRQCD factorization predictions lead to fits to the CDF data that are significantly better than those of the CEM predictions. The normalizations of the CEM predictions are fixed through comparisons with the fixed-target data for charmonium production. Generally, these normalizations are too small. However, even if one adjusts the normalizations so as to optimize the CEM fits to the CDF Tevatron data, the CEM fits are still inferior to the NRQCD factorization fits.

$k_T$  smearing provides a phenomenological model for the effects of multiple gluon emission from the initial-state partons in a hard collision. Its effects are to smooth singularities at  $p_T = 0$  in fixed-order calculations, to increase the predicted cross section at moderately low  $p_T$  (away from the singular region), and to increase the predicted cross section by a smaller amount at high  $p_T$ . Hence, the inclusion of  $k_T$  smearing would be expected to improve the fits of the CEM predictions to the charmonium data, which it does. Even with  $k_T$  smearing, the CEM predictions show substantial disagreement with the data for  $J/\psi$  and  $\chi_c$  production. The smeared NRQCD factorization predictions are in good agreement with the data in all cases. Even if one treats the normalizations of the CEM predictions as free parameters in fitting to the data, the  $k_T$ -smeared CEM predictions result in poorer fits than do the  $k_T$ -smeared NRQCD predictions.

In the case of  $\chi_c$  production, the NRQCD factorization fits are constrained by the relationship of  $\langle \mathcal{O}_1^{\chi_{c0}}(^3P_0) \rangle$  to the corresponding decay matrix element, which, in turn, is constrained by phenomenology. Hence, there is less freedom in this case to tune the matrix elements to obtain a good fit to the data than in the cases of  $J/\psi$  and  $\psi(2S)$  production. The disagreement of the unsmeared NRQCD factorization prediction and the agreement of the smeared NRQCD factorization prediction with the shape of the  $\chi_c$  production data suggests that, if the NRQCD factorization picture is valid, then inclusion of the effects of multiple gluon emission is essential in obtaining the correct shape of the cross section.

Our analysis of the implications of the CEM assumptions for the relative sizes of the nonperturbative NRQCD production matrix elements reveals that the CEM picture for the evolution of a  $Q\bar{Q}$  pair into a quarkonium state is very different from that of NRQCD. Our tentative conclusion, which is subject to caveats about the precision of current theoretical calculations, is that the CEM picture of  $Q\bar{Q}$  evolution into charmonium does not account as well as the NRQCD factorization picture for the slopes, as functions of  $p_T$ , of the charmonium production rates at the Tevatron. Of course, there are large uncertainties in the current theoretical calculations from such sources as higher-order corrections to the CEM and NRQCD factorization predictions. These uncertainties are not reflected in the error bars and  $\chi^2$ 's of the fits, and the corresponding corrections might well affect the shapes of the theoretical predictions. The CEM predictions are very sensitive to the amount of  $k_T$  smearing, while the NRQCD factorization predictions are less sensitive. Hence, a more fundamental calculation of the effects of multiple gluon radiation, such as would be provided by resummations of important logarithms to all orders in  $\alpha_s$ , could help to sharpen the comparison between the predictions of the CEM and the NRQCD factorization picture for quarkonium production at large  $p_T$ .

## Acknowledgments

We thank Ramona Vogt for providing numerical tables of the CEM predictions for charmonium production. We also thank F. Maltoni, M. Mangano, and A. Petrelli for providing their computer codes for calculating the NLO quarkonium cross sections and the evolution of the fragmentation contribution. Work by G. T. Bodwin in the High Energy Physics Division at Argonne National Laboratory is supported by the U. S. Department of Energy, Division of High Energy Physics, under Contract No. W-31-109-ENG-38. E. Braaten is also supported in part by the Department of Energy under grant DE-FG02-91-ER4069. The work of J. Lee was supported by Korea Research Foundation Grant (KRF-2004-015-C00092).

- 
- [1] G. T. Bodwin, E. Braaten, and G. P. Lepage, Phys. Rev. D **51** (1995) 1125 [Erratum-ibid. D **55** (1997) 5853] [hep-ph/9407339].
  - [2] W. E. Caswell and G. P. Lepage, Phys. Lett. B **167** (1986) 437.
  - [3] B. A. Thacker and G. P. Lepage, Phys. Rev. D **43** (1991) 196.
  - [4] N. Brambilla *et al.*, arXiv:hep-ph/0412158.
  - [5] G. C. Nayak, J. W. Qiu, and G. Sterman, arXiv:hep-ph/0501235.
  - [6] H. Fritzsche, Phys. Lett. B **67** (1977) 217.
  - [7] F. Halzen, Phys. Lett. B **69** (1977) 105.
  - [8] M. Gluck, J. F. Owens, and E. Reya, Phys. Rev. D **17** (1978) 2324.
  - [9] V. D. Barger, W. Y. Keung, and R. J. Phillips, Phys. Lett. B **91** (1980) 253; Z. Phys. C **6** (1980) 169.
  - [10] J. F. Amundson, O. J. P. Eboli, E. M. Gregores, and F. Halzen, Phys. Lett. B **390** (1997) 323 [hep-ph/9605295].
  - [11] J. C. Collins and D. E. Soper, Nucl. Phys. B **193**, 381 (1981) [Erratum-ibid. B **213**, 545 (1983)].
  - [12] J. C. Collins and D. E. Soper, Nucl. Phys. B **197**, 446 (1982).
  - [13] E. L. Berger, J. W. Qiu, and Y. L. Wang, hep-ph/0404158.
  - [14] R. Gavai, D. Kharzeev, H. Satz, G. A. Schuler, K. Sridhar, and R. Vogt, Int. J. Mod. Phys. A **10** (1995) 3043 [hep-ph/9502270].
  - [15] G. A. Schuler and R. Vogt, Phys. Lett. B **387** (1996) 181 [hep-ph/9606410].
  - [16] M. L. Mangano, P. Nason, and G. Ridolfi, Nucl. Phys. B **405** (1993) 507.
  - [17] A. Edin, G. Ingelman, and J. Rathsmann, Phys. Rev. D **56** (1997) 7317 [hep-ph/9705311].
  - [18] O. J. P. Eboli, E. M. Gregores, and F. Halzen, Phys. Lett. B **451** (1999) 241 [hep-ph/9802421].
  - [19] O. J. P. Eboli, E. M. Gregores, and F. Halzen, Phys. Rev. D **67** (2003) 054002.
  - [20] O. J. P. Eboli, E. M. Gregores, and J. K. Mizukoshi, Phys. Rev. D **68** (2003) 094009 [hep-ph/0308121].
  - [21] O. J. P. Eboli, E. M. Gregores, and F. Halzen, Phys. Rev. D **64** (2001) 093015 [hep-ph/0107026].
  - [22] E. M. Gregores, F. Halzen, and O. J. P. Eboli, Phys. Lett. B **395** (1997) 113 [hep-ph/9607324].
  - [23] M. Beneke, I. Z. Rothstein, and M. B. Wise, Phys. Lett. B **408**, 373 (1997) [arXiv:hep-ph/9705286].
  - [24] S. Fleming, A. K. Leibovich, and T. Mehen, Phys. Rev. D **68**, 094011 (2003) [arXiv:hep-ph/0306139].

- [25] M. Beneke, arXiv:hep-ph/9703429.
- [26] M. Kramer, Prog. Part. Nucl. Phys. **47**, 141 (2001) [arXiv:hep-ph/0106120].
- [27] F. Abe *et al.* [CDF Collaboration], Phys. Rev. Lett. **79**, 578 (1997).
- [28] R. Vogt, private communication.
- [29] M. L. Mangano, P. Nason, and G. Ridolfi, Nucl. Phys. B **405**, 507 (1993).
- [30] A. Petrelli, private communication.
- [31] A. Petrelli, M. Cacciari, M. Greco, F. Maltoni, and M. L. Mangano, Nucl. Phys. B **514**, 245 (1998) [arXiv:hep-ph/9707223].
- [32] A. D. Martin, R. G. Roberts, W. J. Stirling, and R. S. Thorne, Eur. Phys. J. C **4** (1998) 463 [hep-ph/9803445].
- [33] M. Gluck, E. Reya, and A. Vogt, Eur. Phys. J. C **5**, 461 (1998) [arXiv:hep-ph/9806404].
- [34] P. Cho and A. K. Leibovich, Phys. Rev. **D53** (1996) 6203 [hep-ph/9511315].
- [35] A. D. Martin, W. J. Stirling, and R. G. Roberts, Phys. Lett. B **306** (1993) 145 [Erratum-ibid. B **309** (1993) 492].
- [36] M. Beneke and M. Krämer, Phys. Rev. **D55** (1997) 5269 [hep-ph/9611218].
- [37] H. L. Lai *et al.*, Phys. Rev. D **55** (1997) 1280 [hep-ph/9606399].
- [38] M. Glück, E. Reya, and A. Vogt, Z. Phys. C **67** (1995) 433.
- [39] A. D. Martin, R. G. Roberts, and W. J. Stirling, Phys. Lett. B **387** (1996) 419 [hep-ph/9606345].
- [40] E. Braaten, B. A. Kniehl, and J. Lee, Phys. Rev. D **62** (2000) 094005 [hep-ph/9911436].
- [41] H. L. Lai *et al.* [CTEQ Collaboration], Eur. Phys. J. C **12**, 375 (2000) [arXiv:hep-ph/9903282].
- [42] M. A. Sanchis-Lozano, Nucl. Phys. Proc. Suppl. **86** (2000) 543 [hep-ph/9907497].
- [43] W. K. Tung, *Prepared for International Workshop on Deep Inelastic Scattering and Related Subjects, Eilat, Israel, 6-11 Feb 1994.*
- [44] B. A. Kniehl and G. Kramer, Eur. Phys. J. **C6** (1999) 493 [hep-ph/9803256].
- [45] A. Petrelli, Nucl. Phys. Proc. Suppl. **86** (2000) 533 [hep-ph/9910274].
- [46] K. Sridhar, A. D. Martin, and W. J. Stirling, Phys. Lett. **B438** (1998) 211 [hep-ph/9806253].
- [47] B. Cano-Coloma and M. A. Sanchis-Lozano, Nucl. Phys. **B508** (1997) 753 [hep-ph/9706270].
- [48] F. Maltoni, arXiv:hep-ph/0007003.